

DYNAMIC-PARALLEL MR IMAGE RECONSTRUCTION BASED ON ADAPTIVE COIL SENSITIVITY ESTIMATION

Ke Liu and Jingxin Zhang

Department of Electrical & Computer Systems Engineering, Monash University
Melbourne 3800, Victoria, Australia
ke.liu@eng.monash.edu.au, jingxin.zhang@eng.monash.edu.au

ABSTRACT

Imaging speed is crucial to dynamic Magnetic Resonance Imaging (dMRI) where multiple images must be obtained in a single examination. To accelerate imaging speed, dMRI can be performed with parallel MRI (pMRI) technique by sparsely sampling the k-space of each time frame. However, pMRI reconstruction requires precise estimation of sensitivity maps of receiving coils, which is difficult to obtain with the existing methods. Imperfect estimation of sensitivity maps can dramatically increase artifacts in the reconstructed image. This paper proposes an adaptive sensitivity estimation method to capture the temporal variation of k-space frames and to estimate the unacquired dataset. The estimated dataset is used to create the full k-space for each frame, from which the time varying sensitivity maps are estimated. Experiments on real dynamic-parallel MRI data demonstrate that the proposed method significantly improves the quality of the reconstructed MR images.

Index Terms— Dynamic MRI, parallel MRI, autoregressive model, data estimation.

1. INTRODUCTION

Dynamic Magnetic Resonance Imaging (dMRI) is a widely accepted method in clinical diagnosis and biomedical research. It is used to monitor the function of the patients' organs by sequentially acquiring several images in one particular body area. Similar to conventional MRI, dMRI also suffers from the slow imaging speed problem [3]. To accelerate imaging speed, dMRI is often performed with the parallel MRI (pMRI) technique by sparsely sampling the k-space of each time frame. In order to reconstruct the desired image in pMRI, the coil sensitivity maps are required to unwrap the aliased coil images generated by sparsely sampled k-spaces. Three current methods to acquire coil sensitivity maps in dMRI are : the pre-scanning, temporal average and autocalibration.

Pre-scanning [1] method performs an extra scanning at Nyquist rate on a phantom before or after the dynamic imaging process. Although the pre-scanning method is simple and easy to perform, it has two major drawbacks. Firstly, the sensitivity maps are partially determined by dielectric properties, e.g. susceptibility of the subject to be scanned. Significant changes may occur between the dielectric properties of the phantom used in the extra scan and those of a human body. Secondly, the motion during the dynamic imaging process may change the characteristics of the coil. The temporal average (sliding window) method, [3], [4], uses the sum of every R interleaved undersampled k-spaces to build a new complete k -space, where R is the reduction/acceleration factor. The temporal average method is very efficient and effective in low reduction factor case. However, when a major variation of cardiac position occurs during the respiratory cycle or when a relatively large reduction factor is used, its effectiveness is limited. The loss of information and the inaccuracy of the sensitivity map is proportional to the length of the interval involved in the temporal averaging. In other words, the more frames are used for averaging, the worse the result will be. Furthermore, when the reduction factor R is greater than the number of images N obtained in the imaging process ($R > N$), it is impossible to perform the temporal averaging. In order to cover the central low frequency area, the autocalibration method proposed in [2], integrates the coil sensitivity into the imaging process by including few extra ACS (autocalibration signal) lines. 2D-Fourier Transform of the ACS lines gives a sensitivity-scaled low-resolution and alias-free image. However, the major drawback of this method is the trade-off between the speed of the imaging process and the accuracy of the sensitivity map produced.

In the previous literatures [5],[6], the idea of modeling the variation of the dynamic MRI data over time was exploited. In this paper, we fit multiple AR models to the acquired k - t space data to capture the variation of the time series and to estimate the unacquired Phase-Encoding (PE) lines. Combining the estimated data with the acquired ACS lines, the level of uncertainty in the estimated sensitivity map can be significantly reduced. The main benefit of this approach is the ability to

The authors wish to thank Dr. Peter Kellman, NHLBI, National Institutes of Health, USA, for providing the dataset.

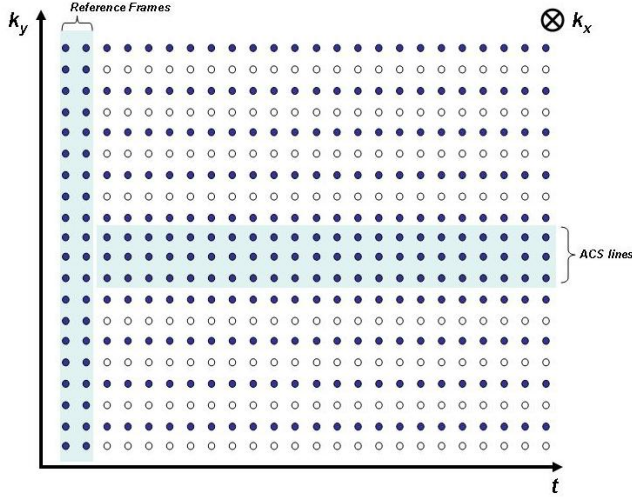


Fig. 1. Sampling Pattern. The dots and circles represent the acquired and skipped PE lines, respectively. Each column represents one time frame.

track the variation of the sensitivity map over time and to provide an updated sensitivity map for each time frame. This time-variation may be caused by respiratory or other physiological motions. Moreover, our approach reduces the examination time by eliminating preliminary training stage.

2. THEORY

2.1. K-T Space Modeling

Fig.1 illustrates the data acquisition scheme used in this paper. According to the proposed sampling pattern, a uniform non-interleaved undersampled k -space is obtained for each dynamic image frame. A complete time series $s_{x,y,l}(n)$ is acquired at (x, y) th pixel of each k -space along the time axis, where n is the discrete time index, x and y are the phase-encoded and frequency-encoded indices respectively ($x = 0, R, 2R, \dots, (M-1)R, y = 0, 1, \dots, N_{fe}, M = \frac{N_{pe}}{R}$), and l is the coil index. In order to learn the temporal properties of the acquired time series, we fit a statistical model, such as AutoRegressive (AR) model to the series $s_{x,y,l}(n)$ at each (x, y, l) position.

Mathematically, learning the properties of the k -space data is a univariate signal description problem, where the observed signal $s_{x,y,l}(n)$ is a time function. A p th-order autoregression model, denoted by $AR(p)$, describes a time-varying signal with the following difference equation:

$$s(n) + a(1)s(n-1) + \dots + a(p)s(n-p) = \varepsilon(n) \quad (1)$$

where p is the maximum time lag between the present and previous data samples $s(n)$ and $s(n-i)$ respectively, $\varepsilon(n)$ is

the residual estimated error with the mean μ and variance σ^2 . The AR parameter is denoted by a_i . The spatial index (x, y) and the coil index l are omitted for simplicity.

Given several observations of the discrete time process data $s(n)$, parameters of the model can be calculated by minimizing the total energy of the residual $E_r = \sum_{n=1}^p \varepsilon^2(n)$. In [7], Burg introduced a preferable estimation method for the AR process. In Burg's algorithm, the residual of the AR process is further expanded to forward and backward residuals with the following definitions:

$$f_m(n) = f_{m-1}(n) + \hat{k}_m b_{m-1}(n-1), \quad (2)$$

$$b_m(n) = b_{m-1}(n-1) + \hat{k}_m f_{m-1}(n), \quad (3)$$

$$n = K+1, \dots, N$$

where $f_m(n)$ and $b_m(n)$ are the forward and backward prediction errors and \hat{k}_m are the reflection coefficients at the m -th stage. The initial conditions for (2) and (3) are $f_0(n) = b_0(n) = s(n)$. The reflection coefficient is iteratively calculated at each stage by minimizing (least squares) the sum of squares of the forward and backward residuals. Taking the partial derivative with respect to the reflection coefficient and equating to zero yields the reflection coefficient at the m -th stage,

$$\hat{k}_K = -2 \frac{\sum_{n=K+1}^N [f_{K-1}(n)b_{K-1}(n-1)]}{\sum_{n=K+1}^N [f_{K-1}^2(n) + b_{K-1}^2(n-1)]} \quad (4)$$

We calculate the AR parameters recursively at each stage from the reflection coefficients k_m through Levinson-Durbin algorithm [7]. The algorithm starts with the initial condition $a_0(0) = 1$ and

$$a_m(n) = a_{m-1}(n-1) + k_m a_{m-1}(n-m), \quad (5)$$

$$n = 1, 2, \dots, m-1$$

to obtain the parameters at the m -th stage. The algorithm repeats for $m = 1, 2, \dots, p$. Finally, the AR parameters obtained at last stage $a_p(n)$ give the desired model parameters a_i in (1).

Next we consider the model order p . An insufficient model order will lead to a fast die out of the estimated data, while over-modeling may result in an unstable model. It was suggested in [7] that the optimized order for a finite-sample process is $N/10$, where N is the length of the time series. However, our experiment shows that a relatively low order model achieves the equivalent performance of a higher order model. For computation simplicity, lower order model is preferred.

2.2. Data Filling and AR Model Based Sensitivity Map Estimation

The k -space data are samples of continuous Fourier transform of the object image. Hence, it is assumed that the time-varying functions are similar for adjacent PE lines. With the

AR model learnt from the full-set k -space data series, the k -space data in adjacent lines can be estimated as follows:

$$\tilde{s}_{x+r}(n) = - \sum_{i=1}^p a_x(i) s_{x+r}(n-i) \quad (6)$$

where $n = 1, 2, \dots, N$, $r = 1, 2, \dots, R-1$, $x = 0, R, 2R, \dots, (M-1)R$ and $\tilde{s}_{x+r}(n)$ is the linear prediction based the learnt AR model from the x -th phase-encoding line. The initial condition $s_{x+r}(0)$ is from the reference frame obtained at the beginning of the examination, where x is the index of the PE lines in the complete k -spaces. In order to create a complete k -space at all time frames of each coil and to fill the blanks between $s_x(n)$ and $s_{x+R}(n)$, the $\tilde{s}_{x+r}(n)$ estimated from (6) are used. These composite k -spaces mixed with both acquired data and estimated data are ready for generating sensitivity-weighted high-resolution and alias-free coil images at each time frame. The sensitivity maps for each time frame are obtained by dividing the coil images by their RSoS image. In the following, the above the estimation method of the sensitivity map will be called the *AR method*.

3. EXPERIMENTAL RESULTS

This section presents the experimental results obtained from a surface coil array dataset. An eight-channel dataset was acquired on a healthy male volunteer in a Siemens 1.5T Avanto scanner with eight-element surface array (Nova Medical, Wilmington, MA). This array had four anterior coils plus four posterior coils.

The dataset was a fully-sampled k - t space. Each frame had 108 phase-encoded and 384 frequency-encoded lines respectively. In order to apply various reduction factors (R), all k -space data were zero-padded to 120 lines in the phase-encoded direction. In all experiments, certain phase-encoded lines were removed to simulate the skipped phase-encoded lines in the real parallel imaging scheme. To avoid the effect of different reconstruction errors caused by various reconstruction algorithms, the SENSE reconstruction scheme was adopted for all methods after the sensitivity maps were estimated. The entire reconstruction process was conducted using MATLAB software.

Three coil calibration methods (pre-scanning, sliding window and autocalibration methods) were compared with the AR model based method at different R . In each cardiac phase, a true image was reconstructed with the "perfect" sensitivity maps, which were generated by the full k -space. For a fair comparison, the efficient reduction factor (R_{eff}) was taken into account in all methods. We define R_{eff} as the ratio of the number of acquired PE lines and the number of total PE lines. For AR and ACS methods, additional central PE lines were kept (a certain number of the these ACS lines overlapped with undersampled k -space PE lines). For the pre-scanning method, the first cardiac frame was fully acquired to simulate the extra scanning usually performed before or after the

dynamic imaging process. For the sliding window method, a sequentially interleaved k - t space sampling scheme was used and the first R frames were summed together to compose a "complete" k space, from which temporal averaged sensitivity maps were extracted. Then the $(R+1)$ th frame along with the previous $R-1$ frames form the next "complete" k space, which will be used to reconstruct the $(R+1)$ th frame and so on.

We present several sequences of reconstructed images using sensitivity maps obtained by different sensitivity map estimation methods. The same reduction factor ($R = 4$) was applied to each of the reconstruction processes and Fig.2 shows four individual frames in a cardiac cycle. In the bottom row of Fig.2, a true image generated by the most accurate sensitivity map was provided for each frame. Compared to the true image, both the pre-scanning and autocalibration methods gave images with strongly visible artifacts, even though 50 ACS lines were used to generate the sensitivity map in the latter. The sliding-window method produced less noise-like effect than the previous two methods; however, because of the inherent drawbacks of the sliding window method, some edge-like artifacts can be observed due to the low temporal resolution of averaged sensitivity maps. Our AR method with only 15 ACS lines provides superior results with less artifacts than all other methods.

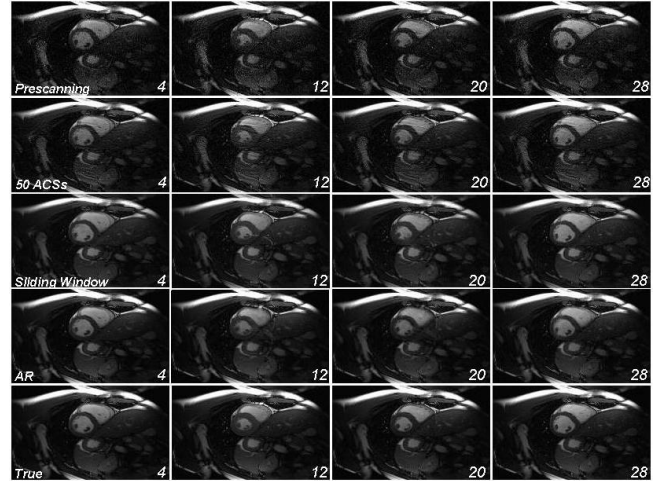


Fig. 2. Four snapshots of the reconstructed image sequences from various sensitivity map estimation methods.

To further verify the effectiveness of the AR method, a critical reduction factor ($R = 8$), was applied to the same 8-channel dataset. In this experiment, pre-scanning and autocalibration methods produced unacceptable reconstruction results with significant artifacts. This is because the high gain of the inverse sensitivity map matrix, due to the very large condition number, magnifies the error caused by the difference between the estimated map and the true sensitivity map. Only the sliding-window and our AR method gives accept-

able reconstructions. As observed from Fig.3, both methods generate reconstruction errors, however, the level of the error is quite different. In Fig.3, the sliding window reconstruction not only has significant error at the border area, but also possesses serious edge-like artifacts in the central region, where the heart locates for both the systole and diastole cases. The error was considerably reduced in AR reconstructions. The AR reconstruction errors are mainly visible in the central region, the most dynamic region during the cardiac cycle. The high-frequency components of k - t space that control the edge of the object were not accurately modeled due to the limited dataset length and this fact accounts for the above observation.

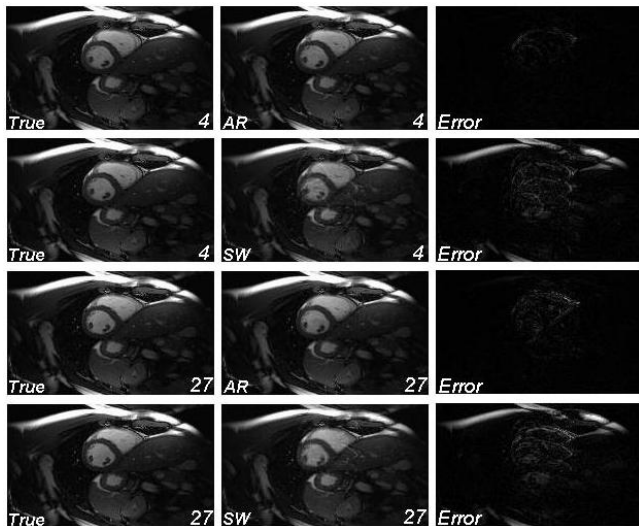


Fig. 3. Comparison of the AR method and sliding window method at $R = 8$ ($R_{eff} = 4.3$). An error and a true image are accompanied with each image to demonstrate the performance of the two methods.

In order to quantify the performance of the two methods, the normalized reconstruction error energy (NREP) is compared in Fig.4. NREP of each cardiac phase is calculated from

$$e_{nml} = \left[\frac{\sum_{i=1}^{N_{pe}} \sum_{j=1}^{N_{fe}} \Delta I_{i,j}}{\sum_{i=1}^{N_{pe}} \sum_{j=1}^{N_{fe}} I_{i,j}} \right]^2 \quad (7)$$

where N_{pe} and N_{fe} are the total numbers of phase-encoded and frequency-encoded lines respectively. $\Delta I_{i,j}$ is the absolute reconstruction error and $I_{i,j}$ is the pixel intensity of the reference image at pixel (i, j) . As expected, our AR method gives much lower NREP at all time frames.

4. CONCLUSION

By using the AutoRegression (AR) model, we have presented a novel sensitivity map estimation scheme to increase the estimation accuracy. The experiments on real dynamic-parallel

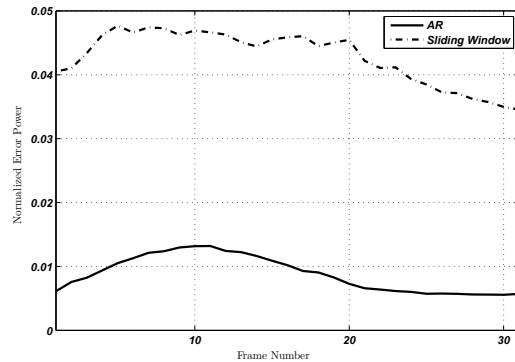


Fig. 4. Normalized error energy at all time frames with reduction factor eight ($R = 8$).

MRI data indicate that the estimation accuracy can be improved by exploiting the temporal correlation existing in k - t space data, which in turn improves the quality of reconstructed images with fewer artifacts.

5. REFERENCES

- [1] K. P. Pruessmann, M. Weiger, M. B. Scheidegger, and P. Boesiger, SENSE: Sensitivity Encoding for Fast MRI. *Magn Reson Med*, vol.42,pp.952-962, 1999.
- [2] P.M. Jakob, M.A.Griswold, R.R. Edelman, D. K. Sodickson. AUTO-SMASH: A self-calibrating technique for SMASH imaging. *Magnetic Resonance Materials in Physics, Biology and Medicine*, vol.7,pp.42-54, 1998.
- [3] P. Kellman, F. H. Epstein, and E. R. McVeigh, Adaptive Sensitivity Encoding Incorporating Temporal Filtering (TSENSE). *Magn Reson Med*,vol.45,pp.846-852, 2001.
- [4] J. Tsao, P. Boesiger, and K. P. Pruessmann, k-t BLAST and k-t SENSE: Dynamic MRI With High Frame Rate Exploiting Spatiotemporal Correlations. *Magn Reson Med*,vol.50,pp.1031-1042, 2003.
- [5] Z. Chen, J. Zhang and K.K.Pang : Adaptive keyhole methods for dynamic magnetic resonance image reconstruction, *Computerized Medical Imaging and Graphics*, Vol. 31, pp. 458-468, 2007.
- [6] C. Prieto, P.G. Batchelor, D.L.G. Hill, J.V. Hajnal, M. Guarini and P. Irarrazaval: Reocnstution of undersampled dynamic images by modeling the motion of object elements. *Magn Reson Med*, vol.57,pp.939-949, 2007.
- [7] P.M.T. Broersen : *Automatic Autocorrelation and Spectral Analysis*. Springer, 2006.